Published in final edited form as:
Int J Radiat Oncol Biol Phys. 2010 June 1; 77(2): 357–366. doi:10.1016/j.ijrobp.2009.04.028.

Intensity-Modulated Proton Therapy Reduces Normal Tissue Doses Compared with Intensity-Modulated Radiation Therapy or Passive Scattering Proton Therapy and Enables Individualized Radical Radiotherapy for Extensive Stage IIIB Non-Small Cell Lung Cancer: A Virtual Clinical Study

Xiaodong Zhang, Ph.D., **Yupeng Li, M.S.**, **Xiaoning Pan, Ph.D.**, **Xiaoqiang Li, M.S.**, **Radhe Mohan, Ph.D.**, **Ritsuko Komaki, M.D.**, **James D. Cox, M.D.**, and **Joe Y. Chang, M.D., Ph.D.**
Division of Radiation Oncology, The University of Texas M. D. Anderson Cancer Center, Houston, TX

Abstract

Purpose—To compare dose-volume histograms (DVHs) for intensity-modulated proton therapy (IMPT) with intensity-modulated radiation therapy (IMRT) and passive scattering proton therapy (PSPT) for stage IIIB non-small cell lung cancer (NSCLC) and explore the possibility of individualized radical radiotherapy.

Methods and Materials—DVHs for IMPT, PSPT, and IMRT designed to deliver IMRT at 60 to 63 Gy, PSPT at 74 Gy, and IMPT at the same doses and individualized radical radiotherapy in patients with extensive stage IIIB NSCLC (N = 10 for each approach) were compared. These patients were selected based on their extensive disease and considered to have no or borderline tolerance of IMRT at 60 to 63 Gy based on normal tissue dose-volume constraints (lung V20<35%, total mean lung dose <20 Gy; spinal cord dose, <45 Gy). The possibility of increasing the total tumor dose with IMPT for each patient without exceeding the dose-volume constraints (maximum tolerant dose, MTD) was also investigated.

Results—Compared with IMRT, IMPT spared more lung, heart, spinal cord, and esophagus even with dose escalation from 63 Gy to 83.5 Gy, with a mean MTD of 74 Gy. Compared with PSPT, IMPT allowed further dose escalation from 74 Gy to mean MTD of 84.4 Gy (range 79.4-88.4 Gy) while keeping all parameters of normal tissue sparing lower or similar. In addition, IMPT prevented lower target coverage in patients with complicated tumor anatomies. Conclusions: IMPT reduces the normal tissue dose and allows individualized radical radiotherapy for extensive stage IIIB NSCLC.

Keywords

Lung cancer; Proton therapy; Intensity-modulated radiation therapy; Passive scattering proton therapy; Intensity-modulated proton therapy

Reprint requests to: Joe Y. Chang, M.D., Ph.D., Department of Radiation Oncology, Unit 97, The University of Texas M. D. Anderson Cancer Center, 1515 Holcombe Blvd., Houston, TX 77030. Tel: (713) 563-2337; Fax: (713) 563-2331; E-mail: jychang@mdanderson.org.

Conflict of Interest Notification: The authors do not have any actual or potential conflicts of interest related to this article.

Introduction

Lung cancer remains the leading cause of cancer-related deaths. About 30% to 40% of patients with locally advanced lung cancer require combined modality treatment including radiotherapy. Conventional photon radiotherapy delivers 60 to 70 Gy using three-dimensional conformal radiotherapy (3-DCRT). However, authors reported that this technique was associated with a 40% to 50% local regional failure rate in stage III non-small cell lung cancer (NSCLC) cases even when concurrent chemotherapy was given (1). Dose escalation can improve local control and possibly survival, but toxicity is a concern, particularly when concurrent chemotherapy is used (1,2). Compared with 3-DCRT, intensity-modulated radiation therapy (IMRT) spares more critical normal tissue and has fewer toxic effects, such as pneumonitis (3,4). However, even with IMRT, significant toxicity is still a dose-limiting factor, particularly for extensive disease such as stage IIIB lung cancer, because of the exit photon dose. Published clinical data using proton therapy showed promising results in stage I NSCLC (5,6). For stage III NSCLC, our previous virtual clinical study demonstrated that proton therapy using a passive scattering approach can further reduce normal tissue doses even with dose-escalated proton therapy (74 Gy) compared with 3-DCRT or IMRT at a conventional dose of 60 Gy (7). Currently, dose-escalated (74 Gy) passive scattering proton therapy (PSPT) with concurrent chemotherapy is used clinically for stage III NSCLC in our institution, and preliminary clinical results have indicated dramatically improved incidence of toxicity, including pneumonitis and esophagitis, compared with our historical data using conventional-dose (60-66 Gy) 3-DCRT and IMRT (8, 2007 PTCOG presentation).

Although PSPT appears to be promising in reducing toxic effects, we are also facing a clinical challenge with dose-escalated radiotherapy using PSPT for lung tumors in very complicated cases, such as contralateral hilum, supraclavicular lymph node involvement, or tumors adjacent to the esophagus and spinal cord. Because of a limited number of treatment fields, delivering ablative doses to targets with complicated shapes or locations, such as tumors curved around sensitive critical structures, is very difficult using PSPT. In such cases, compromised dose coverage has to be considered to avoid damaging critical normal tissue structures. Intensity-modulated proton therapy (IMPT) using scanning beam therapy can simultaneously optimize the intensities and energies of all pencil beams using an objective function that takes into account targets as well as normal tissue constraints. This is the first report of a comparison of dose-volume histograms (DVHs) for IMPT with those for IMRT and PSPT in patients with stage IIIB NSCLC and exploration of the possibility of individualized radical radiotherapy at the maximum tolerated dose (MTD) for this disease.

Methods and Materials

Patients

Twenty patients with inoperable stage IIIB NSCLC were studied. Ten patients actually underwent definitive or palliative radiotherapy (can not tolerate definitive dose) using IMRT in our Thoracic Service, and the remaining 10 actually underwent definitive radiotherapy using PSPT at 74 Gy. The patients in the IMRT group were selected based on the presence of bulky primary tumors with extensive involvement of the contralateral mediastinum and/or hilum and supraclavicular lymph nodes and were considered to have no or borderline tolerance of IMRT at 60 to 63 Gy based on normal tissue dose-volume constraints (volume of lung receiving at least 20 Gy [V20] <35%, total mean lung dose <20 Gy, spinal cord dose <50 Gy). The patients in the PSPT group were selected from among patients enrolled in our dose-escalation (74 Gy) prospective clinical protocol using proton therapy with concurrent chemotherapy. All of 20 patients treated with either IMRT (n=10) or PSPT (n=10) were re-planned using IMPT and compared with actual radiotherapy (IMRT or PSPT, see detail below).

Four-dimensional computed tomography simulation, target delineation, and treatment comparison design

All patients underwent four-dimensional computed tomography (4-DCT) simulation. The gross tumor volume (GTV) was defined as the sum envelope of GTVs extracted from the component images in 10 breath phases. The clinical target volume (CTV) was defined as the GTV plus an 8-mm margin. The planning target volume (PTV) was defined as the CTV plus a 5- to 10-mm margin for IMRT and 5-mm margin for PSPT.

All IMRT and PSPT plans were designed by experienced thoracic dosimetrists and verified by our clinical physicists and our current research team. IMPT plans were designed by our current research team. The lung V20, volume of heart receiving at least 40 Gy (V40), volume of esophagus receiving at least 55 Gy (V55), mean total lung dose, and maximum spinal cord dose were required to be less than 35%, 50%, 50%, 20 Gy, and 45 Gy, respectively. Doses were prescribed for the PTV with at least 95% PTV coverage. Clinically, if an IMRT plan can not meet normal tissue dose-volume criteria, the plan is usually compromised by accepting coverage of less of the target or delivery of a lower target dose. For a fair comparison of IMPT with IMRT, all IMRT plans were renormalized with at least 95% PTV coverage to 63 Gy.

For each patient, an individualized IMPT plan was designed to reach the maximum tolerant dose (MTD), defined as maximal deliverable dose without exceeding normal tissue dose-volume constraints as stated above plus additional constraints of less than 80 Gy for the esophagus and less than 74 Gy for 5 cc of the esophagus because the esophagus was considered a dose-limiting structure. Those plans were referred to as IMPT_MTD plans. For IMPT_MTD plan, we first prescribed PTV to ablative dose of 90 Gy and then optimized the treatment plan based on PTV coverage and normal tissue dose-volume constraints. Since esophagus was the major dose limiting critical structure for IMPT plan after initial optimization, the IMPT optimizer continued to sacrifice the PTV coverage until the esophagus dose volume constrains have been met. After these optimizations converged, we chose the dose covering 95% PTV as the MTD for the patient. To compare the IMPT and IMRT plans, the IMPT isodose distributions and DVHs were analyzed at 63 Gy and the MTD. To compare the IMPT and PSPT plans, the IMPT isodose line distributions and DVHs were analyzed at 74 Gy and the MTD.

IMRT, PSPT, and IMPT planning methods

IMRT and PSPT were planned as we described previously (3-5,9). The dosimetric data for the IMRT plan were extracted from the clinically administered and approved plans using the Pinnacle radiation therapy planning system (Philips Medical Systems, Bothell, WA), whereas the dosimetric data for the PSPT plan were obtained from the clinically administered and approved plans using the Eclipse proton therapy planning system (Varian Medical Systems, Inc., Palo Alto, CA). The typical PSPT three-field arrangement was used for all of the plans. For each proton field, a block was designed to shape the field laterally, and a compensator was designed to shape the distal end of the dose distribution conformal to the distal surface of the target. The treatment plans were designed based on the CTV using parameters similar to those described by Moyers et al. (10). The typical smearing margin for the range compensator was 1 cm to account for setup uncertainties. The border-smoothing width was the same as the aperture margin.

The IMPT plans were designed using the Eclipse proton therapy planning system with the dynamic beam-scanning system at our institution. To achieve the optimum dose coverage of the target and spare the region of interest, a multifield optimization (MFO) approach was used in which all of the spot intensities were simultaneously optimized based on an objective function taking into account target as well as normal tissue constraints. The optimization process consisted of the following steps: 1) selection of the beam-field directions, 2)

determining the minimal and maximal energy layer and all intermediate energies for the field, 3) arrangement of the spot positions for each energy layer, 4) calculation of the start weights for each spot, 5) selection of the dose-volume objectives, 6) calculation of the dose deposition matrix, 7) performance of the optimization, 8) post-processing to convert the raw spot weights calculated using the optimizer to the physical characteristics of the treatment unit, and 9) calculation of the final dose distributions.

The maximum and minimum energies for each beam were determined using the distal margin (DM) and proximal margin of the PTV. All intermediate energies between the maximum and minimum energies preconfigured during the commissioning process were selected for the optimization. The spots for each energy layer were arranged in a fixed two-dimensional spot grid. The dimension of this two-dimensional grid was determined by the target and its lateral margins (LMs). Conventionally, the LMs were selected based on the penumbra of the lateral dose profile. However, because the intensity of the beam spots at the periphery of the targets could be increased to compensate for the penumbra margin, a tight LM of 0.4 cm was used. Also, although the spot spacing could be optimized, fixed spot spacing was used. The initial values of the spot weights for each energy layer were set so that they would lead to a flat spread-out Bragg peak under ideal conditions.

The inverse planning process for IMPT is very similar to that for IMRT. The treatment planner can interactively adjust the dose, volume, and penalty of each objective for each region of interest, including the PTV. In our study, the TPS implemented gradient-based simultaneous spot optimization and conjugated gradient optimization algorithms. A simultaneous spot optimization algorithm was used for all of the IMPT plans. Prior to optimization, the inverse planning system calculated the dose deposition coefficients matrix. For this matrix, the dose that would be deposited to each of the voxels when irradiating each single spot with a unit intensity was calculated. Calculating the dose deposition coefficients matrix normally took longer than optimization time during the entire IMPT planning process. After completion of the optimization process, the Eclipse system was used to perform post-processing, which is the step that adapts the raw spot weights calculated by the optimizer to the physical characteristics of the treatment unit. Because the maximum and minimum MU for the scanning beam delivery system are 0.040 and 0.005, respectively, the major post-processing includes layer repainting, which is division of delivery of the dose coming from an individual energy layer into several repetitions. The “cut and append” option was used to perform the repainting. Given the layer spot weight list, Eclipse goes through the list; when a spot weight exceeds 0.04 MU, it is truncated to 0.04 MU, and the spot with the rest of the weight is appended at the end of the list. The resulting spot list may contain the same spot position several times, but all spot weights are lower than or equal to 0.04 MU If the MU of the spot is smaller than the minimum MU, the weight of the spot is rounded down to 0 or up to the 0.005 MU. After post-processing, the dose was recalculated. In this sense, the final spot weight and positions were deliverable using our system.

Results

IMPT produced lower normal tissue doses than IMRT and allowed delivery of radical doses to targets

Compared with the IMRT plans, the IMPT plans spared more of the contralateral and ipsilateral lung, heart, spinal cord, and esophagus (Table 1). A typical case of comparison is shown in Fig. 1: we compared the isodose distributions for IMRT and IMPT at 63 Gy in a patient with stage IIIB NSCLC. In this patient, the mean lung dose for IMRT and IMPT was 29.0 Gy and 20.0 Gy, respectively, and the maximum spinal cord dose for IMRT and IMPT was 47.2 Gy and 45.0 Gy, respectively. The actual IMRT plan did not meet our normal tissue dose-volume constraints (mean lung dose <20 Gy and maximum spinal cord dose <45 Gy), but the IMPT

plan did. Table 1 shows the dose-volume data comparing IMRT (60-63 Gy), IMPT (63 Gy), and IMPT_MTD for the 10 patients. Again, while keeping the PTV coverage similar, IMPT spared more of the lung (19.8% mean absolute improvement in total volume of lung receiving at least 5 Gy [V5], 27% mean absolute improvement in contralateral lung V5), heart (14.2% mean absolute improvement in heart V40), esophagus (6.8% mean absolute improvement in esophageal V55), and spinal cord (9.5 Gy mean absolute improvement in spinal cord maximal dose) than IMRT did (Table 1).

More importantly, IMPT allowed radiation dose escalation from 63 Gy up to 83.5 Gy with a mean MTD of 74 Gy in this selective group of patients with extensive stage IIIB disease; the same cases were considered to be borderline treatable or unable to tolerate administration of 63 Gy using IMRT according to the same dose-volume constraints (see Methods and Materials). Even with IMPT_MTD, IMPT improved all normal tissue-sparing parameters except for the esophageal V55, which was similar to that of IMRT at 63 Gy (Table 1). Fig. 2 shows a comparison of IMPT_MTD at 80 Gy with IMRT at 63 Gy in a single patient.

IMPT produced lower normal tissue doses than PSPT did and allowed further dose escalation beyond 74 Gy)

As shown in Fig. 3 and 4, because of the proximity of the spinal cord to the CTV and PTV, the PSPT aperture must be modified to meet the normal tissue dose-volume constraints. As a consequence, we found that the CTV/PTV coverage was compromised and that the intended 74-Gy dose was not delivered to all of the CTV using PSPT. Fig. 4 shows the isodose line distributions for PSPT and IMPT at 74 Gy in the same patient with stage IIIB NSCLC. The spinal cord was clearly spared using a curved dose distribution, which is a characteristic of IMPT, without compromising the PTV coverage. For this patient, because we could use overlapping beams with IMPT, we avoided passage of proton beams through large areas of lung tissue. As a result, we achieved much better lung sparing with the IMPT plans than with the PSPT plans. The improved lung, esophageal, and spinal cord sparing with IMPT is reflected in the DVH shown in Fig. 4.

Because we considered 74 Gy to be the close to MTD for acute and chronic side effects in the esophagus, further dose escalation beyond 74 Gy is limited using PSPT in our patients with stage IIIB NSCLC because of the proximity of target volumes such as the mediastinal lymph nodes to the esophagus. Also, a quite common event in patients such as ours is that sparing of the esophagus conflicts with target coverageas discussed above. However, IMPT has a planning advantage over PSPT, particularly with complicated tumor anatomies. Table 2 shows the dose-volume data from a comparison of the PSPT (74 Gy), IMPT (74 Gy), and IMPT_MTD plans in the 10 patients. The MTD using IMPT for the PTV based on the normal tissue dose-volume constraints was 84.4 Gy (range, 79.4-88.4 Gy). Compared with PSPT, IMPT allowed further dose escalation to close to ablative doses while maintaining lower or similar normal tissue-sparing parameters. Again, IMPT allowed us to administer treatment to patients with complicated tumor anatomies and ensure adequate PTV coverage without increasing normal tissue toxicity.

Discussion

The 5-year survival rate for stage IIIB NSCLC is only 5% to 10% after conventional definitive radiotherapy (60-63 Gy) and chemotherapy. Among them, about 50% recurred locally. Also, uncontrolled local disease may continue to seed to distant organs, resulting in distant metastasis. Dose escalation to 74 Gy may improve local control and possibly survival rates. However, delivery of 74 Gy may not be possible without damaging surrounding critical structures in many cases of stage IIIB NSCLC. PSPT provides the unique opportunity to allow dose escalation to 74 Gy in this particular group of patients. However, in select cases, such as

a patient with a curved target or a target proximal to at least one critical structure, compromised target coverage must be considered to reduce the toxicity. In addition, 74 Gy may not be a high enough dose to eliminate all disease, particularly for bulky lesions. Clinical studies have indicated that use of a higher dose is correlated with improved local control and survival rates if patients can tolerate the treatment (2). Physical characteristics of protons beam and unique treatment planning advantage of IMPT over IMRT and PSPT may enable the use of ablative doses (>74 Gy) for stage IIIB NSCLC. The present virtual clinical study supported this hypothesis, as we found that normal tissue doses using IMPT at even ablative doses up to 88.4 Gy were lower than those using IMRT at 60 to 63 Gy or PSPT at 74 Gy. IMPT_MTD may translate to better clinical tumor control and survival and fewer side effects using individualized IMPT-mediated radical radiotherapy compared with PSPT and IMRT. The clinical benefit of these dosimetric improvements remains to be validated in prospective clinical trials. The National Institutes of Health has approved and supported with a program grant to conduct prospective clinical studies including phase I/II clinical protocols designed to study individualized radical dose escalation using IMPT in stage III NSCLC in a collaboration between Massachusetts General Hospital and our institution.

Similar to the PSPT plans, we used two to four beams for the IMPT plans. However, IMPT has several advantages over PSPT, particularly with a complicated tumor anatomy. Fig. 3a shows the three-beam PSPT plan, and Fig. 3b shows the beam-eye view of the posterior oblique beam of PSPT. For the PSPT plan, we edited the aperture to avoid the spinal cord, which compromised the PTV coverage. Clinically, we observed cases of local failure of PSPT because of marginal target missing resulting from the compromised coverage. However, using the same beam direction with the IMPT plan, we spared the spinal cord via inverse planning. Fig. 3c shows the dose distribution for PSPT when we used two significantly overlapping beams. Because the PSPT plan does not use a wedge or other beam-modifying device, we could see the large area of the hot region. As shown in Fig. 3d, the hot region resulting from the overlap of the two PSPT beams could be mitigated using inverse IMPT planning.

Using IMPT, we could judiciously select the DM to take advantage of modulation of the scanning beams. It is well known that inhomogeneities in the path of a proton beam may significantly degrade its distal edge. Degradation of one beam may be compensated by depositing doses using pencil beam or spots of beams from different directions. This is illustrated schematically in Fig. 5. Panel A shows a single lateral IMPT beam passing through a textured lung-like medium with an average ρ value of 0.2 gm/cc. After passing through the target, it enters a uniform medium with a ρ value of 0.2 gm/cc. Degradation of the distal edge of the proton beam, although exaggerated by the low density of the latter medium, is obvious and corresponds with the dose profile along the horizontal axis (the blue line in panel C of Fig. 5). However, this degradation may be mitigated by IMPT. As shown in panel B of Fig. 5, we added anterior-posterior (AP) and posterior-anterior (PA) IMPT beams and gave the lateral beam a negative DM. This optimization process compensated for the resulting loss of target coverage by adjusting the energies and intensities of the pencils of the AP and PA beams. The resulting dose profile along the horizontal axis is indicated by the solid red line in panel C of Fig. 5; the dashed red line is the renormalized (to 100% at the isocenter) contribution of the lateral beam to the total dose represented by the solid red line. These explained the dosimetric advantages of IMPT over PSPT in cases with complicated tumor anatomies.

As we know, the main challenge with IMPT for lung cancer is organ and tumor motion. We previously showed that about 50% of lung tumors move 0.5 to 1 cm and that 10% move more than 1 cm (11). Motion control procedures such as breath holding and gated treatment for tumors that move more than 1 cm should be considered. Also, a four-dimensional proton therapy plan is required when taking tumor motion into consideration (12). In our institution, 4DCT simulation is required for evaluation of organ and tumor motion in all patients who

undergo proton therapy. In addition to breath holding or gated treatment, we previously showed that use of the four-dimensional internal gross tumor volume with maximal density projection override with an average CT data set for compensator and aperture design provided better target coverage while sparing more of critical normal structures than did other approaches (13). In addition to intrafraction tumor motion, interfraction motion and anatomic changes may dramatically alter the radiation dose distribution (9,14). All of these issues should be considered and resolved in administering proton therapy, particularly IMPT, for lung cancer. However, in most cases (90%), lung tumors move less than 1 cm. Particularly for Stage IIIB NSCLC, the tumor is more extensive and usually attached to a mediastinal structure, and has much less tumor motion compared with stage I disease although it can still move more than 1 cm in some cases (11,15).

Although IMPT has shown great advantages over PSPT in reducing dose to normal tissues and potential dose escalation in treating very advanced lung tumors, the interplay effect of dynamic delivery and tumor motion must be considered. However, the interplay effect during scanning beam delivery may be averaged out by dose repainting in fractionated IMPT (16). Finally, IMPT may be the last therapeutic resort for patients who cannot tolerate dose escalation or even conventional doses of radiation given using IMRT or PSPT.

Conclusions

IMPT may reduce the normal tissue dose and allow further dose escalation in patients with extensive stage IIIB NSCLC who cannot tolerate or have borderline tolerance of standard-dose radiotherapy using IMRT or PSPT. Individualized MTD irradiation using IMPT with normal tissue dose-volume constraints appears feasible in this group of patients and may lead to improved local tumor control. Prospective clinical trial is needed to validate the data.

Acknowledgments

We thank all members of the thoracic radiation oncology and Proton Therapy Center teams at M. D. Anderson Cancer Center for their help and support. We thank the Department of Scientific Publications at M. D. Anderson for their assistance in the preparation of this article.

Dr. Chang is a recipient of the Research Scholar Award from the Radiological Society of North America and a Project Development Award from the M. D. Anderson National Institutes of Health Lung Cancer SPORE. This research was supported in part by grant R01-CA74043 and P01-CA 021239 from the National Cancer Institute. The abstract was presented during the 2008 Particle Therapy Co-Operative Group (PTCOG) and 2008 American Society for Therapeutic Radiology and Oncology annual meetings.

References

1. Curran W, Scott C, Langer C, et al. Long term benefit is observed in a phase III comparison of sequential vs concurrent chemo-radiation for patients with unresectable NSCLC: RTOG 9410. Proc Am Soc Clin Oncol 2003:621a.
2. Kong F, Ten Haken R, Schipper M, et al. High-dose radiation improved local tumor control and overall survival in patients with inoperable/unresectable non-small-cell lung cancer: Long-term results of a radiation dose escalation study. Int J Radiat Oncol Biol Phys 2005;63:324–333. [PubMed: 16168827]
3. Murshed H, Liu H, Liao Z, et al. Dose and volume reduction for normal lung using intensity-modulated radiotherapy for advanced-stage non-small-cell lung cancer. Int J Radiat Oncol Biol Phys 2004;58:1258–1267. [PubMed: 15001271]
4. Yom S, Liao Z, Liu H, et al. Initial evaluation of treatment-related pneumonitis in advanced- stage non-small-cell lung cancer patients treated with concurrent chemotherapy and intensity-modulated radiotherapy. Int J Radiat Oncol Biol Phys 2007;68:94–102. [PubMed: 17321067]
5. Bush DA, Slater JD, Shin BB, Cheek G, Miller DW, Slater JM. Hypofractionated proton beam radiotherapy for stage I lung cancer. Chest 2004;126(4):1198–1203. [PubMed: 15486383]

6. Widescott L, Amichetti M, Schwarz M. Proton therapy in lung cancer: linical outcomes and technical issues. A systematic review Radiother Oncol 2008;86(2):156–164.

7. Chang JY, Zhang X, Wang X, et al. Significant reduction of normal tissue dose by proton radiotherapy compared with three-dimensional conformal or intensity-modulated radiation therapy in Stage I or Stage III non-small-cell lung cancer. Int J Radiat Oncol Biol Phys 2006;65:1087–1096. [PubMed: 16682145]

8. Cox JD, Chang JY, Liao Z, et al. Acute esophageal reactions from proton beam therapy and concurrent chemotherapy for NSCLC: Reduction in incidence and severity despite higher doses. J Thorac Oncol 2007;2:S449.

9. Hui Z, Zhang X, Starkschall G, et al. Effects of interfractional motion and anatomic changes on proton therapy dose distribution in lung cancer. Int J Radiat Oncol Biol Phys 2008;72:1385–1395. [PubMed: 18486357]

10. Moyers MF, Miller DW, Bush DA, et al. Methodologies and tools for proton beam design for lung tumors. Int J Radiat Oncol Biol Phys 2001;49:1429–1438. [PubMed: 11286851]

11. Liu HH, Balter P, Tutt T, et al. Assessing respiration-induced tumor motion and internal target volume using 4DCT for radiation therapy of lung cancer. Int J Radiat Oncol Biol Phys 2007;68:531–540. [PubMed: 17398035]

12. Engelsman M, Rietzel E, Kooy HM. Four-dimentional proton treatment planning. Int J Radiat Oncol Biol Phys 2006;64:1589–1595. [PubMed: 16580508]

13. Kang Y, Zhang X, Chang JY, et al. 4D Proton treatment planning strategy for mobile lung tumors. Int J Radiat Oncol Biol Phys 2007;67:906–914. [PubMed: 17293240]

14. Lomax AJ. Intensity modulated proton therapy and its sensitivity to treatment uncertainties 2: The potential effects of inter-fraction and inter-field motions. Phys Med Biol 2008;53:1043–1056. [PubMed: 18263957]

15. Ezhil M, Vedam S, Balter P, et al. Determination of patient-specific internal gross tumor volumes for lung cancer using four-dimensional computed tomography. Radiat Oncol 2009;4 in press.

16. Bortfeld T, Jokivarsi K, Goitein M, Kung J, Jiang SB. Effects of intra-fraction motion on IMRT dose delivery: Statistical analysis and simulation. Phys Med Biol 2002;47:2203–2220. [PubMed: 12164582]

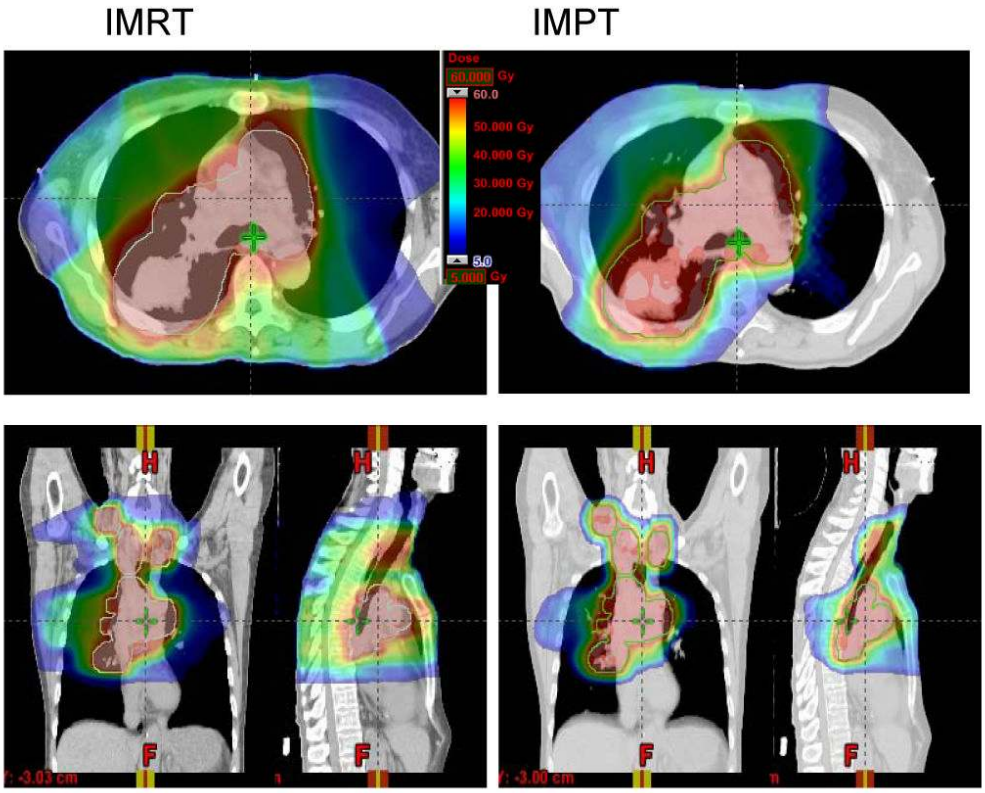

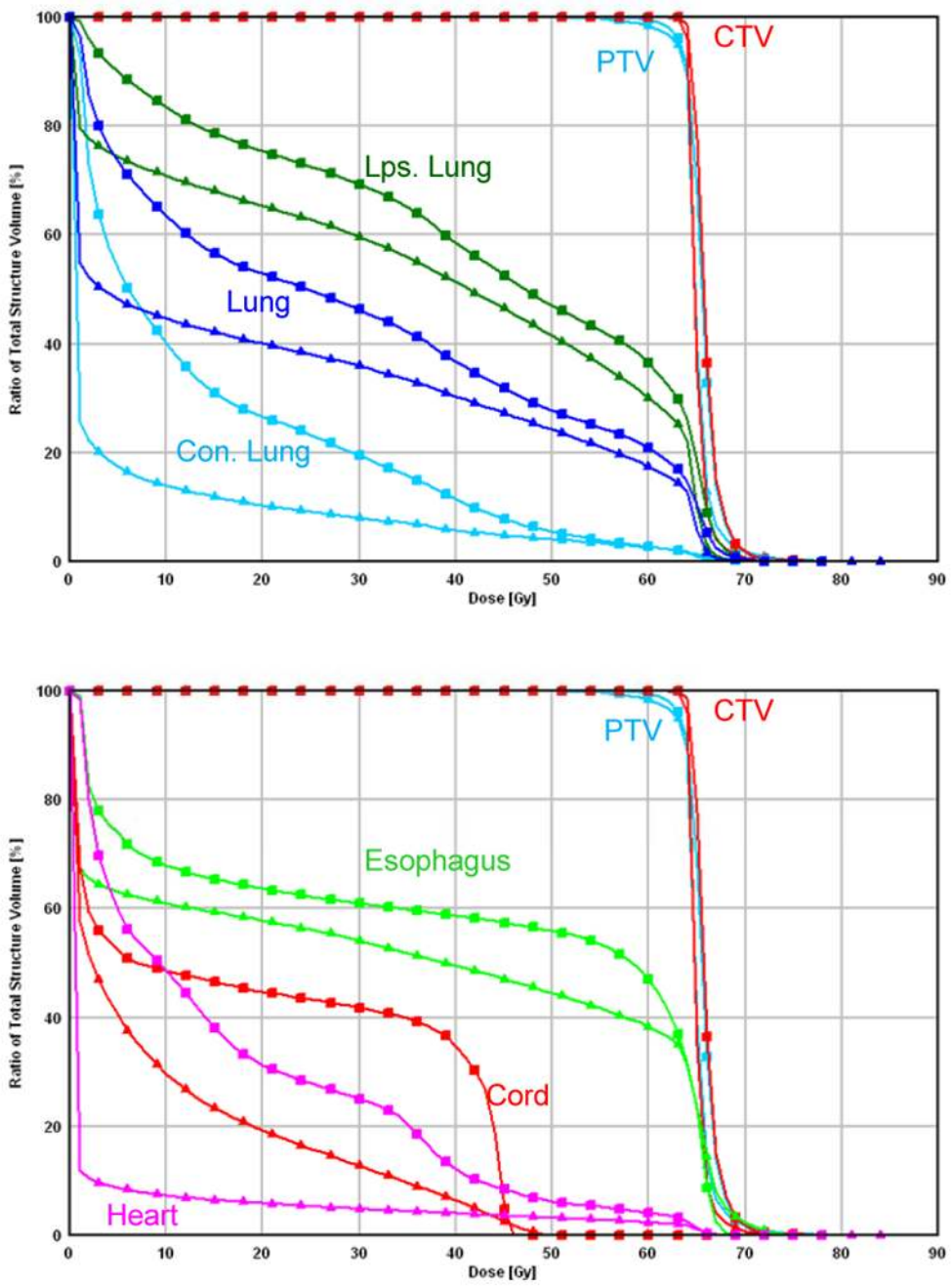

Fig. 1.

A typical case comparison between IMRT and IMPT. (a) Dose distributions for the IMRT (left) and IMPT (right) plans. Each line delineates the PTV. (b) DVHs for the IMRT plan (squares) and IMPT plan (triangles). Ips., ipsilateral; Con., contralateral.

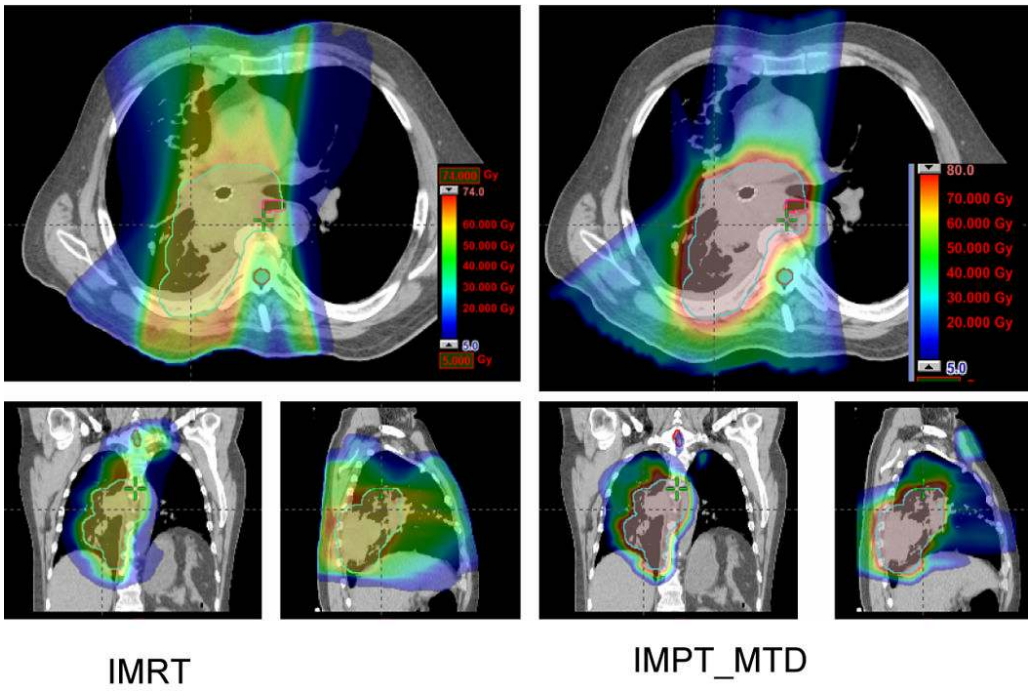

IMRT IMPT_MTD

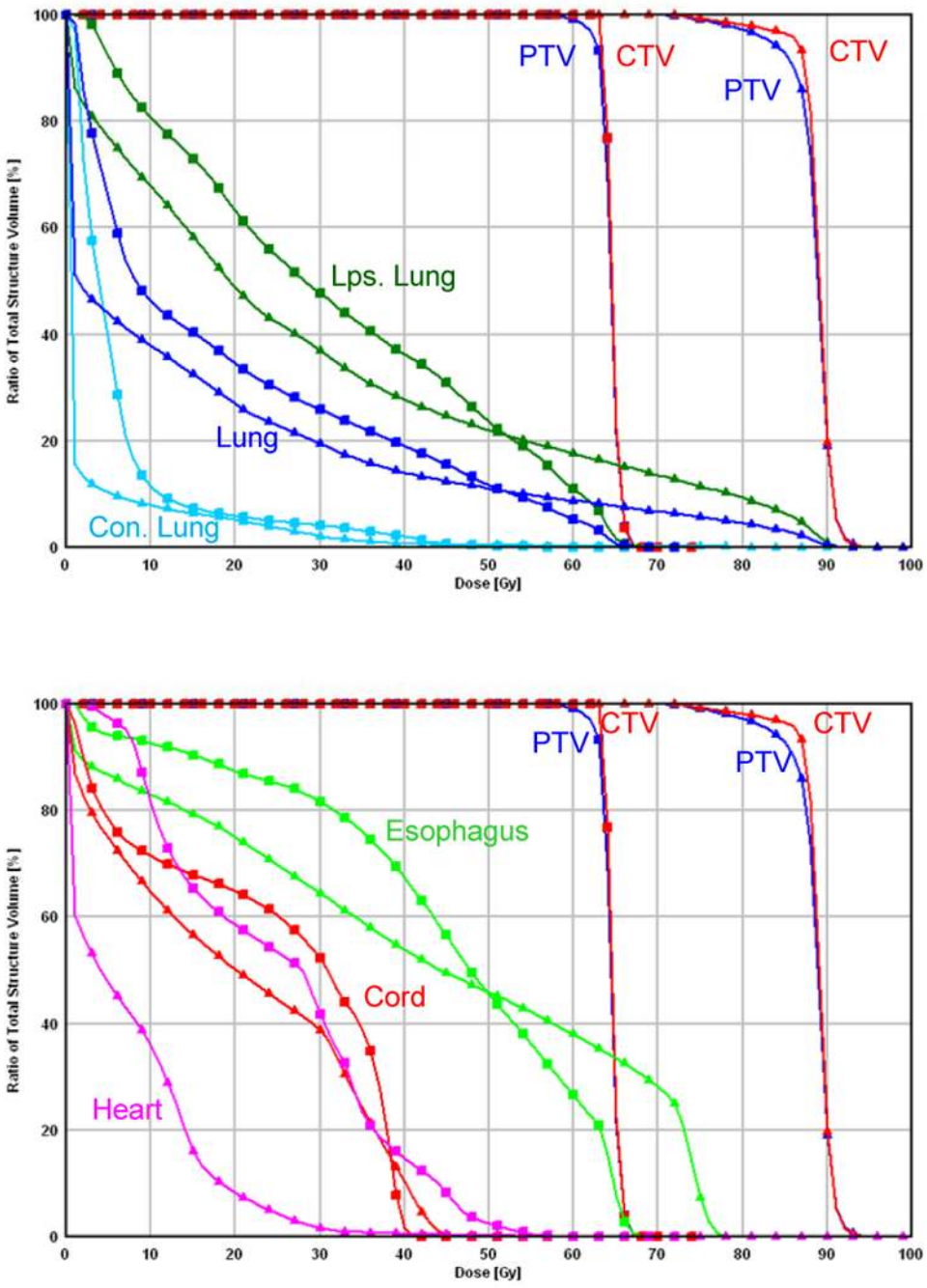

Fig. 2.

Comparison between IMRT and IMPT_MTD. (a) Dose distributions for the IMRT plan at 63 Gy (left) and IMPT_MTD plan at the MTD of 80 Gy (right). Each line delineates the PTV. Of note is that the esophagus was overlapped by the CTV and PTV for this patient, whereas the IMPT_MTD plan was able to reduce the esophageal dose to less than 80 Gy. (b) DVHs for the IMRT plan (squares) and IMPT_MTD plan (triangles). Ips., ipsilateral; Con., contralateral.

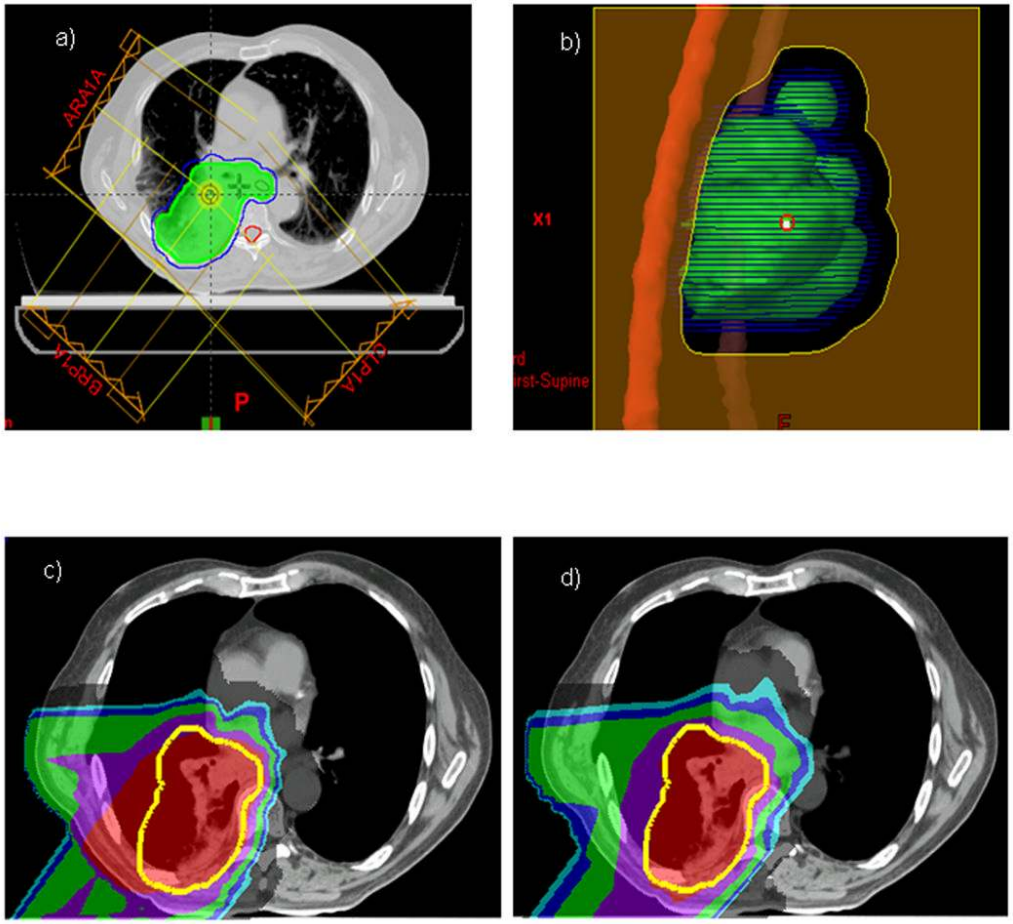

Fig. 3.

Comparison of IMPT with PSPT in treating an NSCLC lesion close to the spinal cord. (a) Beam arrangements for a typical PSPT plan. (b) Beam-eye view of the aperture block, CTV (green contour), PTV (blue contour), and spinal cord (red contour) for the right lateral beam. The aperture had to be edited for this beam to avoid the cord. (c) The hot region resulting from the overlap of the two beams for the PSPT plan. CTV: yellow contour. (d) Avoidance of the hot region by intensity modulation for the IMPT plan with the use of the same two beams.

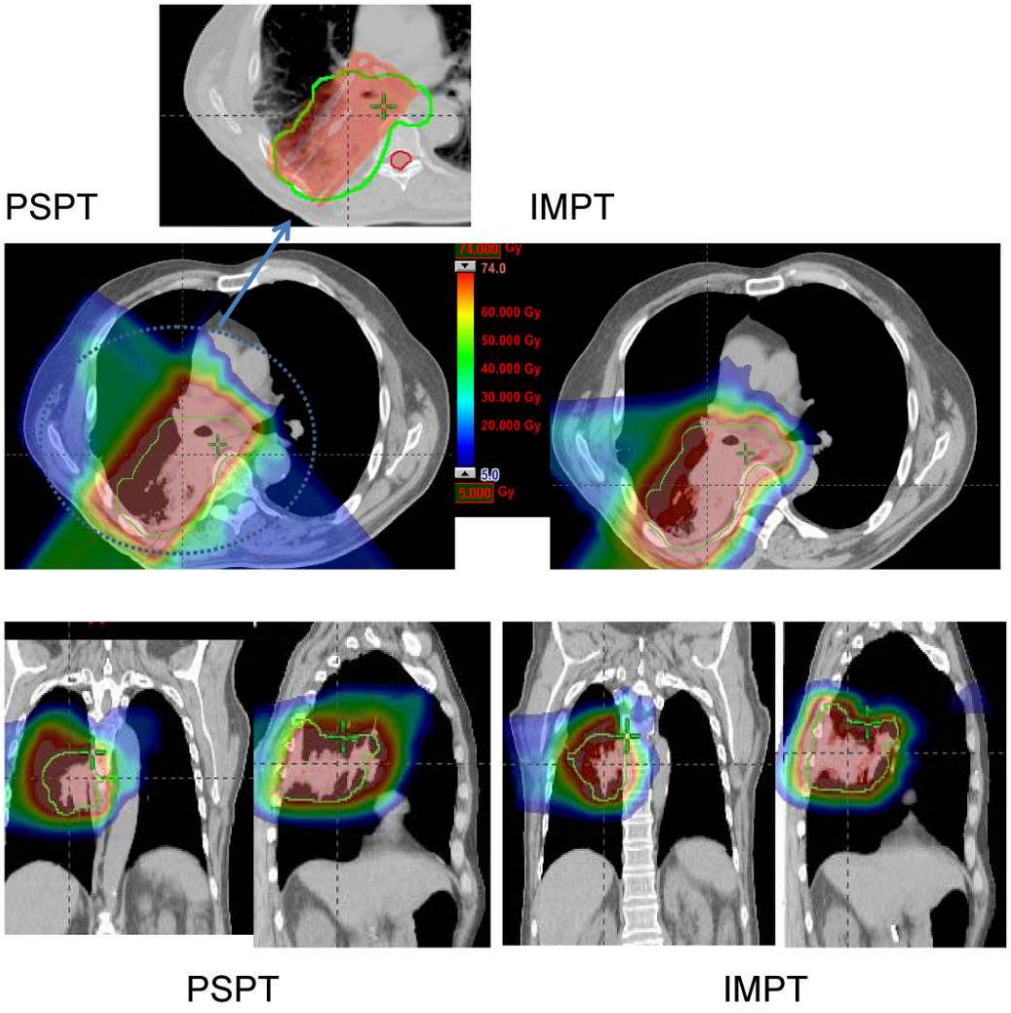

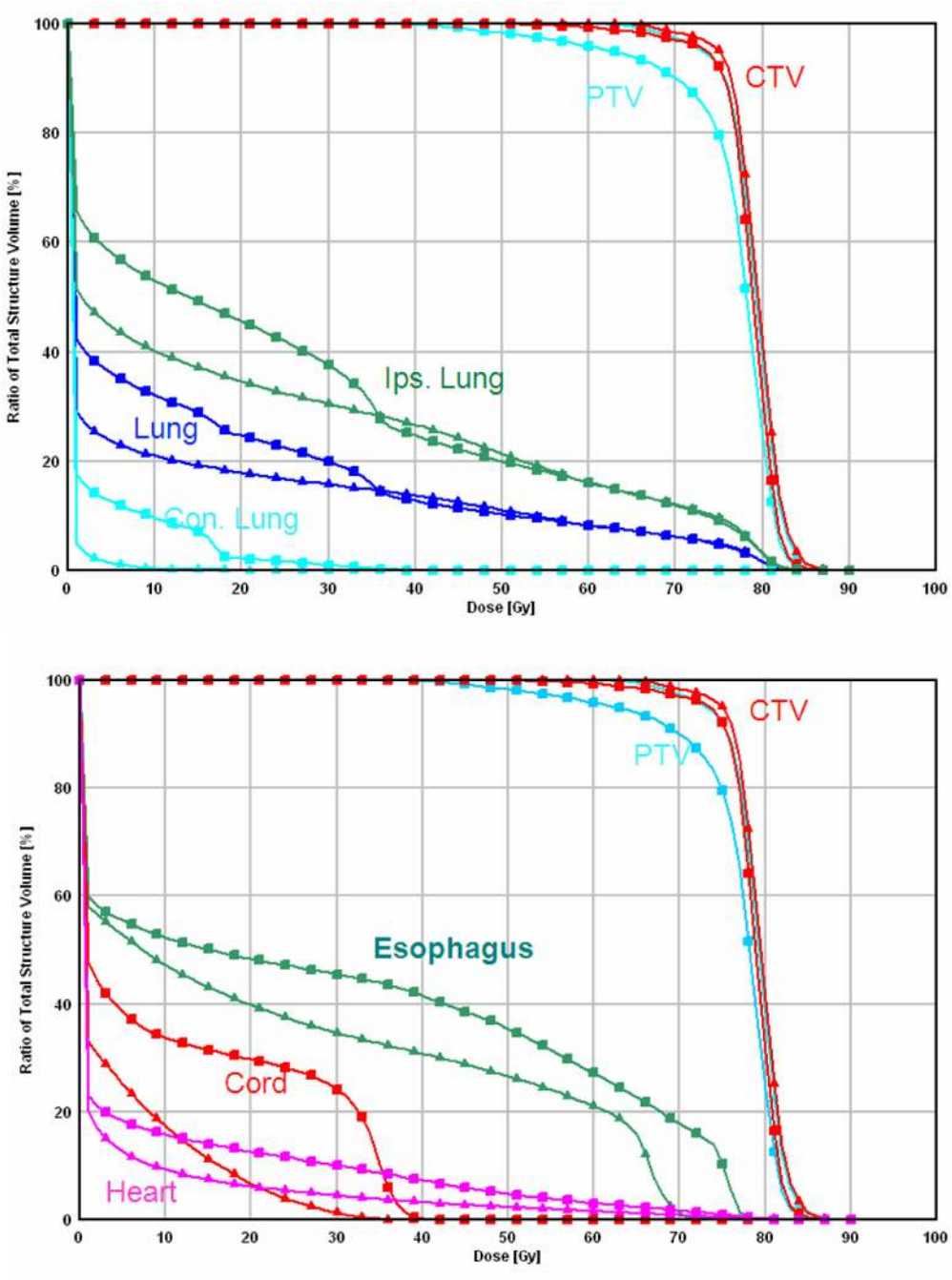

Fig. 4.

Comparison between PSPT and IMPT. (a) Dose distributions for the PSPT (left) and IMPT (right) plans. The green lines delineate the PTV. A blown-up image of the target region for the PSPT is shown to indicate the inadequate dose coverage caused by aperture editing. (b) DVHs for the PSPT plan (squares) and IMPT plan (triangles). Ips., ipsilateral; Con., contralateral.

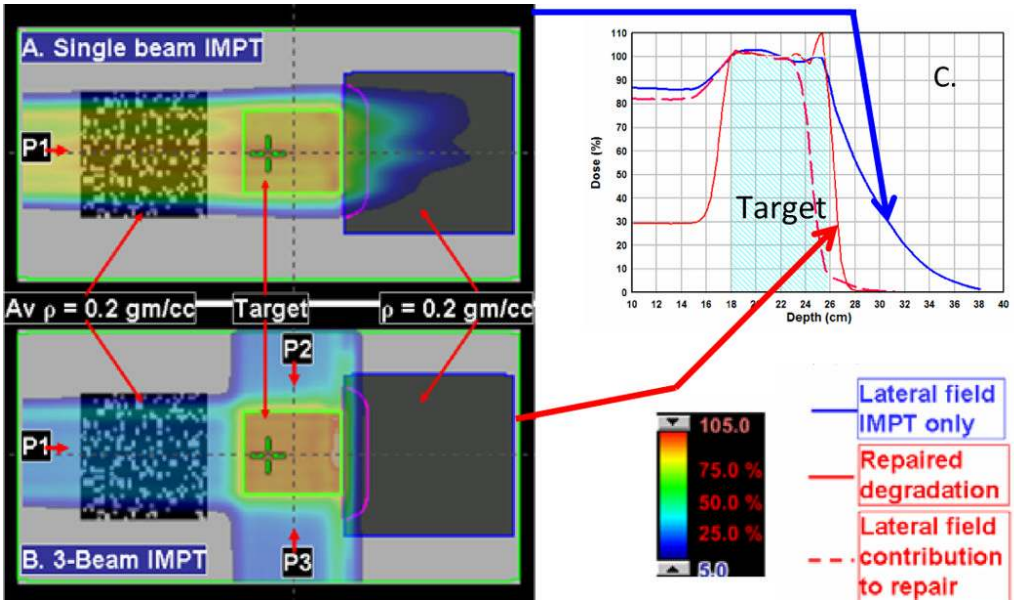

Fig. 5.

IMPT bean degradation repair by depositing doses from different directions. (A) A single lateral IMPT beam passing through a textured lung-like medium with an average ρ value of 0.2 gm/cc. After passing through the target, the beam enters a uniform medium with a ρ value of 0.2 gm/cc. The degradation of the distal edge of the beam corresponds to the dose profile along the horizontal axis (the blue line in panel C). If the beam had passed through a uniform low-density medium upstream, the degradation would not have occurred. (B) The addition of AP and PA IMPT beams and use of a negative margin for the lateral beam to deposit no more than 10% of its maximum dose distal to the target. (C) The optimization process compensated for the resulting loss of target coverage by adjusting the energies and intensities of the pencils of the AP and PA beams. The resulting dose profile along the horizontal axis is indicated by the solid red line in panel C. The dashed red line is the renormalized (to 100% at the isocenter) contribution of the lateral beam to the total dose represented by the solid red line.

Table 1

Medians and ranges of endpoint values in the IMRT, IMPT and IMPT_MTD plans. V5. volume (of lung) exposed to 5 Gy or more; d1, dose received by 1% (of the spinal cord).

		IMRT (range)	IMPT (range)	IMPT_MTD (range
Total Lung	V5 (%)	58.6 (38.7-73.3)	38.8 (27.4-48.2)	39.5 (28.4-47.7)
	V10 (%)	45.3 (31.6-63.5)	34.4 (24.5-44.7)	35.5 (25.8-44.2)
	V20 (%)	34.6 (23.7-52.9)	27.6 (20.3-40.0)	29.3 (22.4-39.3)
	V30 (%)	28.6 (19.4-46.2)	22.5 (14.2-35.9)	24.3 (18.5-34.6)
	Mean (Gy)	20.0 (14.1-29.2)	15.0 (10.8-21.9)	17.1 (13.9-20.4)
Con. Lung	V5 (%)	48.8 (33.0-80.7)	21.8 (2.7-63.5)	22.4 (2.9-63.5)
	V10 (%)	31.3 (10.6-68.7)	18.3 (1.2-59.9)	19.0 (1.3-59.9)
	V20 (%)	20.1 (2.2-56.4)	13.0 (0.2-53.3)	14.3 (0.3-53.3)
	V30 (%)	14.7 (0.6-50.5)	9.8 (0.0-42.8)	10.7 (0.0-42.8)
	Mean (Gy)	12.6 (4.6-33.2)	7.2 (0.5-27.4)	7.9 (0.5-27.4)
Ips. Lung	V5 (%)	68.0 (39.3-91.9)	54.4 (24.3-82.2)	55.5 (25.4-82.9)
	V10 (%)	58.5 (34.0-84.0)	49.4 (18.9-76.4)	50.9 (20.1-77.8)
	V20 (%)	48.3 (20.3-75.4)	40.9 (12.6-65.3)	43.2 (13.9-64.4)
	V30 (%)	41.6 (15.5-69.3)	34.1 (8.4-59.7)	36.9 (10.0-60.1)
	Mean (Gy)	26.9 (13.2-41.9)	22.3 (6.6-37.2)	25.7 (7.7-40.1)
Spinal Cor	dDmax (Gy)	45.5 (36.8-50.4)	36.0 (18.9-53.0)	40.9 (19.0-54.2)
	D1 (Gy)	43.5 (35.7-48.1)	30.5 (16.0-47.2)	34.5 (15.9-44.1)
Heart	V40 (%)	21.8 (0.0-70.4)	7.6 (0.0-26.0)	8.0 (0.0-27.0)
Esophagus	V40 (%)	46.3 (24.8-67.4)	38.1 (9.6-51.3)	42.9 (16.4-56.2)
	V55(%)	32.2 (9.7-53.5)	25.4 (2.0-41.7)	32.9 (8.7-45.5)

Table 2

Medians and ranges of endpoint values in the PSPT, IMPT and IMPT_MTD plans.

		PSPT (range)	IMPT (range)	IMPT_MTD (range)
Total Lung	V5 (%)	37.1 (18.4-45.1)	31.8 (14.4-43.6)	32.3 (14.7-46.5)
	V10 (%)	33.5 (17.0-42.7)	28.2 (12.5-40.1)	29.1 (13.0-42.3)
	V20 (%)	27.4 (14.5-35.9)	23.4 (9.6-33.7)	24.8 (10.1-36.0)
	V30 (%)	21.9 (9.5-31.0)	18.6 (8.2-26.3)	20.5 (8.7-26.6)
	Mean (Gy)	15.8 (7.1-22.4)	13.1 (6.4-18.7)	15.3 (7.3-20.4)
Con. Lung	V5 (%)	10.0 (0.3-24.7)	5.7 (0.0-18.8)	6.9 (0.0-22.7)
	V10 (%)	7.3 (0.1-16.9)	4.3 (0.0-15.3)	5.2 (0.0-18.4)
	V20 (%)	3.6 (0.0-9.5)	2.6 (0.0-10.0)	3.5 (0.0-13.5)
	V30 (%)	1.8 (0.0-7.5)	0.8 (0.0-3.6)	1.3 (0.0-4.7)
	Mean (Gy)	2.2 (0.1-6.2)	1.2 (0.0-4.4)	1.6 (0.0-5.6)
Ips. Lung	V5 (%)	62.5 (33.8-86.6)	56.3 (26.8-83.0)	56.3 (27.3-84.2)
	V10 (%)	58.2 (31.5-83.6)	50.9 (23.2-79.1)	51.7 (24.0-80.1)
	V20 (%)	50.2 (26.9-77.6)	43.3 (17.8-71.2)	45.1 (18.7-71.5)
	V30 (%)	41.5 (17.6-70.5)	36.1 (15.2-62.2)	39.0 (16.1-61.3)
	Mean (Gy)	29.0 (13.2-49.3)	24.7 (11.8-41.5)	28.5 (13.5-43.8)
Spinal Cord	Dmax (Gy)	34.2 (26.4-43.2)	35.9 (17.8-49.0)	37.1 (8.1-58.1)
	D1 (Gy)	28.5 (19.0-39.4)	26.8 (4.8-43.0)	24.5 (4.6-43.2)
Heart	V40 (%)	10.1 (0.0-33.7)	9.3 (0.0-28.0)	10.0 (0.0-29.5)
Esophagus	V40 (%)	26.8 (0.0-47.9)	24.2 (0.0-43.1)	25.1 (0.0-44.2)
	V55(%)	18.4 (0.0-37.0)	16.1 (0.0-30.6)	18.4 (0.0-32.7)